

Latest Results on Standard Candle Central Exclusive Production within the Durham Model

^a L.A. Harland-Lang ^b

Cavendish Laboratory, University of Cambridge, J.J. Thomson Avenue, Cambridge, CB3 0HE, UK

V.A. Khoze

Department of Physics and Institute for Particle Physics Phenomenology, University of Durham, DH1 3LE, UK

M.G. Ryskin

Petersburg Nuclear Physics Institute, Gatchina, St. Petersburg, 188300, Russia

W.J. Stirling

Cavendish Laboratory, University of Cambridge, J.J. Thomson Avenue, Cambridge, CB3 0HE, UK

The latest results on standard candle central exclusive production (CEP) processes within the pQCD based Durham model are discussed, which involve the production of systems with sufficiently low masses that observation of these processes is already possible at the Tevatron and in the early LHC low pile-up runs. The CEP of the χ_c meson is in particular addressed, concentrating on the $\chi_c \rightarrow \pi^+\pi^-$ channel. The continuum background to this process is calculated, which requires a careful treatment of both the ‘perturbative’ and ‘non-perturbative’ contributions, and is found to be under control once suitable cuts are imposed on the final state pions. The CEP of other meson pairs, such as flavour-singlet states, which have much larger predicted cross sections than in the case of $\pi^+\pi^-$ CEP, is also discussed.

1 Introduction

There has recently been a renewal of interest in studies of central exclusive production (CEP) processes in high-energy proton-(anti)proton collisions, both theoretically and experimentally, see for instance ^{1,2,3,4}. The CEP of an object X may be written in the form

$$pp(\bar{p}) \rightarrow p + X + p(\bar{p}), \quad (1)$$

where + signs are used to denote the presence of large rapidity gaps. An important advantage of these reactions is that they provide an especially clean environment in which to measure the nature and quantum numbers (in particular, the spin and parity) of new resonance states, from ‘old’ SM mesons to BSM Higgs bosons ^{5,6,7,8,9,10,11}. One of the most interesting examples is the CEP of the Higgs boson, which is at the heart of the FP420 LHC upgrade project ¹²: through the installation of dedicated forward proton detectors 420m away from the ATLAS and/or CMS detectors, it is hoped that detailed studies of new physics in high-luminosity runs of the LHC can be performed.

^aKRYSTHAL collaboration

^bspeaker

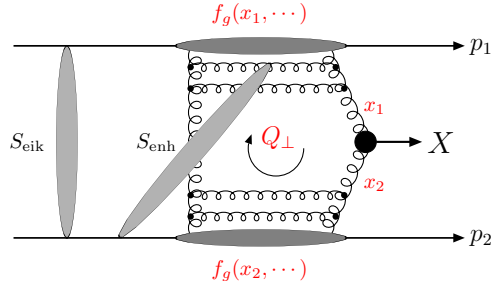


Figure 1: The perturbative mechanism for the exclusive process $pp \rightarrow p + X + p$, with the eikonal and enhanced survival factors shown symbolically.

As discussed in detail in for example^{6,8}, the CEP of, for instance, $\gamma\gamma$, heavy (c, b) quarkonia, new charmonium-like states or meson pairs with sufficiently large p_\perp can serve as ‘standard candle’ processes with which we can benchmark predictions for new CEP physics at the LHC, as well as offering a promising way to study various aspects of QCD.

The formalism used to calculate the perturbative CEP cross section (see Fig. 1) is explained in detail elsewhere^{5,6,7,8}. The expected cross sections and final-state particle distributions (in particular of the outgoing protons) are determined by a non-trivial convolution of the hard amplitude T and the so-called soft survival factors S^2 , defining the probability that the rapidity gaps survive soft and semi-hard rescattering effects⁴. This is modelled in the SuperCHIC Monte Carlo¹³, which allows for an exact generation on an event-by-event basis of the distributions of the final-state central particles and outgoing protons, as well as a precise evaluation of the expected acceptances after experimental cuts have been imposed.

Recently the LHCb Collaboration has reported preliminary results on the CEP of χ_c mesons in the $\chi_c \rightarrow J/\psi + \gamma$ channel, where vetoing was imposed on additional activity in the rapidity region $1.9 < \eta < 4.9$, with some sensitivity to charged particles in the backwards region $-4 < \eta < -1.5$ ¹⁴. While the $\chi_{c(0,1)}$ production data are in good agreement with the theoretical predictions for exclusive production^{5,6}, the observed χ_{c2} rate is somewhat higher. However, it is worth recalling that the observed LHCb data include some fraction of events with proton dissociation. In⁸ qualitative arguments were given that the protons dissociative process should favour the production of higher spin $\chi_{c(1,2)}$ states, with the χ_{c2} yield being particularly enhanced. However a more accurate account of the effects caused by the un-instrumented regions in the LHCb experiment¹⁴ requires more detailed quantitative studies^c, and this is addressed elsewhere¹⁵.

Another way to help clarify the situation, as discussed in^{5,6,17,18}, is to consider other decay modes, with the observation of χ_{c0} CEP via two-body decay channels to light mesons ($\pi^+\pi^-$, K^+K^- , $p\bar{p}$...) represents an interesting and realistic possibility. Considering the case of $\chi_c \rightarrow \pi^+\pi^-$ CEP for example, while the χ_{c0} cross section is of the same size as in the $\chi_{c0} \rightarrow J/\psi\gamma \rightarrow \mu^+\mu^-\gamma$ channel, the fact that the $\chi_{c(1,2)}$ two-body branching ratios are in general of the same size or smaller (or even absent for the χ_{c1}) than for the χ_{c0} , ensures that the $J_z = 0$ selection rule is fully active, see^{5,17} for more details. However, in this case we may in principle expect a sizeable background resulting from direct QCD $\pi^+\pi^-$ production; such a non-resonant contribution should therefore be carefully evaluated. This process can be modelled in two different ways, depending on the phase space region being considered: for low invariant mass and/or transverse momentum final states a ‘non-perturbative’ mechanism, calculated using the tools of Regge theory, should dominate, while the high k_\perp tail of the $\pi^+\pi^-$ CEP process should be generated by a purely pQCD mechanism, which cannot be predicted within the framework of Regge theory. We will discuss each of these in turn.

^cOn the experimental side, the addition of FSCs on both sides of the LHCb experiment¹⁶ would allow a more efficient veto on inelastic events and should greatly clarify the situation.

2 Non-perturbative CEP mechanism

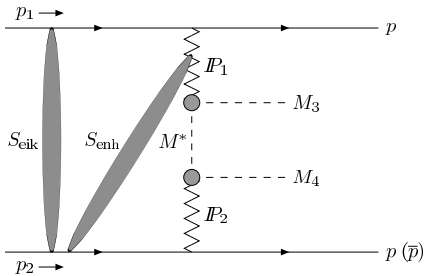


Figure 2: Representative diagram for the non-perturbative meson pair (M_3, M_4) CEP mechanism, where M^* is an intermediate off-shell meson of type M . Eikonal and (an example of) enhanced screening effects are indicated by the shaded areas.

In the low mass (low k_\perp) region, we expect a non-perturbative picture of the type shown in Fig. 2 to give the dominant contribution. For this one-meson-exchange mechanism^{18,19,20}, the meson ($\pi^+\pi^- \dots$) pair is created via double-Pomeron exchange, with an intermediate t -channel off-shell meson. The amplitude is calculated using the tools of Regge theory, which we summarise here, see^{8,15} for more details. The CEP matrix element is given by $\mathcal{M} = \mathcal{M}_{\hat{t}} + \mathcal{M}_{\hat{u}}$, with $\hat{t} = (P_1 - k_3)^2$, $\hat{u} = (P_1 - k_4)^2$, where P_i is the momentum transfer through Pomeron i , and $k_{3,4}$ are the meson momenta. We have

$$\mathcal{M}_{\hat{t}} = \frac{1}{M^2 - \hat{t}} F_p(p_{1\perp}^2) F_p(p_{2\perp}^2) F_M^2(\hat{t}) \sigma_0^2 \left(\frac{s_{13}}{s_0} \right)^{\alpha(p_{1\perp}^2)} \left(\frac{s_{24}}{s_0} \right)^{\alpha(p_{2\perp}^2)}, \quad (2)$$

where M is the meson mass and $s_{ij} = (p'_i + k_j)^2$ is the c.m.s. energy squared of the final state proton-meson system (ij). The normalisation is set by the total meson-proton cross section $\sigma(\pi p) = \sigma_0 (s_{ij}/s_0)^{\alpha(0)-1}$. The factor $F_M(\hat{t})$ in (2) is the form factor of the intermediate off-shell meson and, as discussed in⁸, it is quite poorly known, in particular for larger values of \hat{t} . It seems reasonable to take a typical ‘soft’ exponential form $F_M(\hat{t}) = \exp(b_{\text{off}}(\hat{t} - M^2))$, and the value of the slope can be approximately fitted to reproduce the correct normalisation of CERN-ISR data²¹. A reasonable fit is given by the choice $b_{\text{off}} = 0.5 \text{ GeV}^{-2}$.

Finally, we have to include an additional suppression factor to calculate the genuinely exclusive cross section, i.e. that due to screening corrections, which in terms of the Reggeon formalism are described by the exchange of additional (one or more) Pomerons. First, there is the exchange between the two incoming (outgoing) protons (p_1, p_2), which is just the usual eikonal survival factor S_{eik} . While we in principle also have to consider exchanges between the protons and the $PIP \rightarrow M_3 \bar{M}_4$ system, these effects are expected to be suppressed by the smallness of triple-Pomeron coupling²², and the small size of the produced mesons $\sim 1/\sqrt{\hat{s}}$ which gives a very small meson-proton absorptive cross section in the phase space region we will consider. Next, we recall that there is no secondary interaction between two outgoing mesons mediated by Reggeon exchange. This can be seen as follows: since the meson pair production time in Fig. 2 is practically instantaneous ($\sim 1/E$), while a much longer time ($\sim E/m^2$) is needed for the formation of a Reggeon by the secondary meson, there is insufficient time for a Reggeon emitted by one meson to interact with the other. Following⁸, we introduce an extra suppression of the form of $\exp(-n)$, corresponding to the small Poisson probability not to emit other secondaries in the $PIP \rightarrow M_3 \bar{M}_4$ process at the initial meson pair production stage. Here $n(s_{M\bar{M}})$ is the mean number of secondaries. This factor may be described as the reggeization of the M^* meson exchange, which means that we now deal with non-local meson-Pomeron vertices and the t -channel meson M^* becomes a non-local object, i.e. it has its own size. It is this non-locality that is responsible for the non-violation of causality.

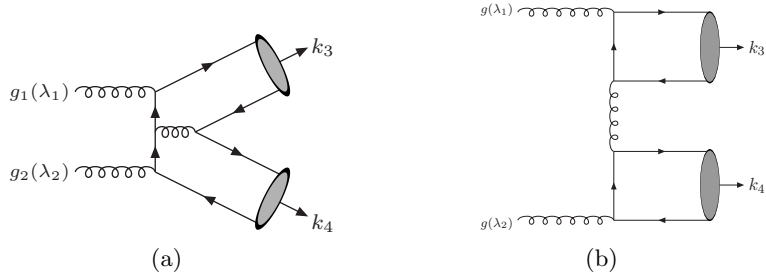


Figure 3: (a) A typical diagram for the $gg \rightarrow M\bar{M}$ process. (b) Representative ‘ladder’ diagram, which contributes to the production of flavour-singlet mesons.

3 Perturbative CEP mechanism

At higher values of the meson k_{\perp} we can model the meson pair CEP process using the pQCD–based Durham model, as in Fig. 1. To calculate the $gg \rightarrow M\bar{M}$ subamplitude we use a generalisation of the ‘hard exclusive’ formalism used to calculate the $\gamma\gamma \rightarrow M\bar{M}$ cross section at wide angles^{23,24}. The amplitude can be written in the form

$$\mathcal{M}_{\lambda\lambda'}(\hat{s}, \theta) = \int_0^1 dx dy \phi_M(x) \phi_{\bar{M}}(y) T_{\lambda\lambda'}(x, y; \hat{s}, \theta). \quad (3)$$

where \hat{s} is the $M\bar{M}$ invariant mass, x, y are the meson momentum fractions carried by the quarks, λ, λ' are the gluon helicities and θ is the scattering angle in the gg cms frame. $T_{\lambda\lambda'}$ is the $gg \rightarrow q\bar{q}q\bar{q}$ hard scattering amplitude, where each (massless) $q\bar{q}$ pair is collinear and has the appropriate colour, spin, and flavour content projected out to form the parent meson.

We can then calculate the relevant parton-level helicity amplitudes for the $gg \rightarrow M\bar{M}$ process, for the production of scalar flavour-nonsinglet meson states ($\pi\pi, K^+K^-, K^0\bar{K}^0$). There are seven independent Feynman diagrams to compute– a representative diagram is given in Fig. 3 (a). An explicit calculation gives⁸

$$T_{gg}^{++} = T_{gg}^{--} = 0, \quad (4)$$

$$T_{gg}^{+-} = T_{gg}^{-+} = \frac{\delta^{AB}}{N_C} \frac{64\pi^2 \alpha_S^2}{\hat{s}xy(1-x)(1-y)} \frac{(x(1-x) + y(1-y)) N_C}{a^2 - b^2 \cos^2 \theta} \frac{N_C}{2} \left(\cos^2 \theta - \frac{2C_F}{N_C} a \right), \quad (5)$$

where A, B are colour indices and

$$a = (1-x)(1-y) + xy \quad b = (1-x)(1-y) - xy. \quad (6)$$

We can see that the $gg \rightarrow M\bar{M}$ amplitude for $J_z = 0$ gluons (4) vanishes at LO for scalar flavour-nonsinglet mesons, which, recalling the $J_z = 0$ selection rule²⁵ that strongly suppresses the CEP of non- $J_z = 0$ states, will lead to a strong suppression (by \sim two orders of magnitude) in the CEP cross section. As a result, we may expect the perturbative contribution to the continuum background to $\chi_c \rightarrow \pi^+\pi^-$ to be small. We can also see that the $|J_z| = 2$ amplitude (5) vanishes for a particular value of $\cos^2 \theta$. This vanishing of a Born amplitude for the radiation of massless gauge bosons, for a certain configuration of the final state particles is a known effect, usually labelled a ‘radiation zero’²⁶. The destructive interference effects which lead to the zero in the $|J_z| = 2$ amplitude (5) will tend to further suppress the CEP rate. A further important consequence of this is that the $\pi^0\pi^0$ QCD background to the $\gamma\gamma$ CEP process described above is predicted to be small. In²⁸ CDF reported the observation of 43 $\gamma\gamma$ events with $|\eta(\gamma)| < 1.0$ and $E_T(\gamma) > 2.5$ GeV, with no other particles detected in $-7.4 < \eta < 7.4$, which corresponds to a cross section of $\sigma_{\gamma\gamma} = 2.48_{-0.35}^{+0.40}$ (stat) $_{-0.51}^{+0.40}$ (syst) pb. The theoretical cross section, calculated

using the formalism described in⁶ and implemented in the SuperCHIC MC generator¹³, is 1.42 pb using MSTW08LO PDFs²⁹ and 0.35 pb using MRST99 (NLO) PDFs³⁰, while the p_{\perp} , $\Delta\phi$ and invariant mass distributions of the $\gamma\gamma$ pair are well described by the MC. In the analysis in²⁸ special attention was paid to the possible background caused by $\pi^0\pi^0$ CEP, since one or both of the photons from $\pi^0 \rightarrow \gamma\gamma$ decay can mimic the ‘prompt’ photons from $gg \rightarrow \gamma\gamma$ CEP. Importantly, CDF has found that the contamination caused by $\pi^0\pi^0$ CEP is very small (< 15 events, corresponding to a ratio $N(\pi^0\pi^0)/N(\gamma\gamma) < 0.35$, at 95% CL), supporting this result.

It is also possible for the $q\bar{q}$ forming the mesons to be connected by a quark line, via the process shown in Fig. 3 (b). These amplitudes will only give a non-zero contribution for the production of $SU(3)_F$ flavour-singlet states, i.e. $\eta'\eta'$ and, through $\eta\text{--}\eta'$ mixing, $\eta\eta$ and $\eta\eta'$ production. The explicit amplitudes are given elsewhere⁸, but the crucial result is that the $J_z = 0$ amplitudes do not vanish as in the case of flavour non-singlet mesons, and so we will expect $\eta'\eta'$ CEP to be strongly enhanced relative to, for example, $\pi\pi$ production, due to the $J_z = 0$ selection rule which operates for CEP. In the case of $\eta\eta$ production, the flavour singlet contribution will be suppressed by a factor $\sin^4\theta_P \sim 1/200$, where θ_P is the octet-singlet mixing angle²⁷, which may therefore be comparable to the $|J_z| = 2$ flavour-octet contribution. In fact, after an explicit calculation we find that the $\eta\eta$ CEP cross section is expected, in the regions of phase space where the perturbative formalism is applicable, to be dominant over $\pi\pi$ CEP. As $\eta^{(\prime)}\eta^{(\prime)}$ CEP is expected to have larger perturbative cross sections it may therefore represent an experimentally more realistic and theoretically cleaner (that is, with a smaller non-perturbative contribution) observable.

4 $\chi_{c0} \rightarrow \pi^+\pi^-$: perturbative and non-perturbative contributions

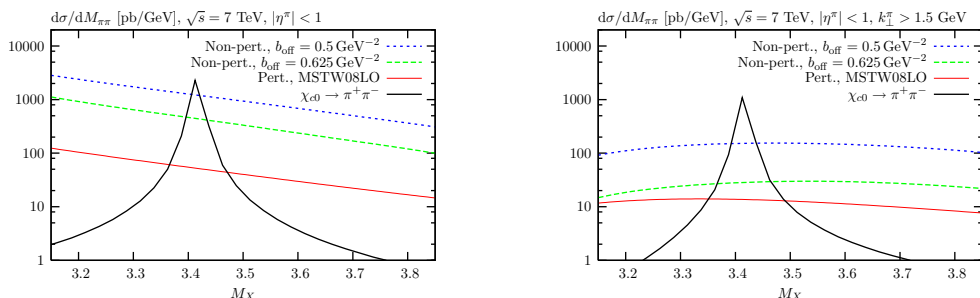


Figure 4: $\chi_{c0} \rightarrow \pi^+\pi^-$ Breit-Wigner peak, and perturbative and non-perturbative (for different b_{off} values) contributions to non-resonant $\pi^+\pi^-$ CEP in the χ_{c0} mass region at $\sqrt{s} = 7$ TeV, for different k_{\perp} and η cuts on the pions.

Finally, in Figs. 4 we show results for the $\pi^+\pi^-$ CEP cross section at $\sqrt{s} = 7$ TeV in the χ_{c0} mass region, which will be relevant for evaluating the potential continuum background to resonant $\chi_{c0} \rightarrow \pi^+\pi^-$ production. The $\pi^+\pi^-$ mass distribution from χ_{c0} decay is given by a simple non-relativistic Breit-Wigner, with the χ_{c0} cross section normalisation set using the SuperCHIC MC¹³, which implements the theory described in⁶. We can see that once basic η cuts are imposed on the final state pions, the χ_{c0} signal is expected to lie at a similar level to the non-perturbative background with $b_{\text{off}} = 0.5 \text{ GeV}^{-2}$, and that the perturbative contribution is expected to be negligible. Although we note that the non-perturbative background may be somewhat lower in this mass region (for comparison we also show the background for the choice $b_{\text{off}} = 0.625 \text{ GeV}^{-2}$, which gives a lower cross section), it is not completely clear that the signal peak will be visible over the background, taking into account the theory uncertainties (experimental resolution effects may also decrease the S/B ratio). However, if we also impose a $k_{\perp} > 1.5 \text{ GeV}$ cut on the pions, we can see that the background is further reduced with little

effect on the χ_c signal rate (for which the χ_c mass $M_{\chi} \approx 3.5$ GeV ensures that a large fraction of the central pions have $k_{\perp} > 1.5$ GeV): the predicted $\chi_{c0} \rightarrow \pi^+\pi^-$ rate lies (at least) an order of magnitude above the expected background. We can therefore safely conclude that even within the (in principle quite large) theory uncertainties, $\chi_{c0} \rightarrow \pi^+\pi^-$ is expected to represent a clean experimental signal, with a low continuum background once suitable cuts are imposed.

To conclude, studies in ^{5,6,7,8} demonstrate the rich phenomenology that CEP processes offer at high-energy colliders. We have concentrated here on the case of meson pair CEP, and in particular the potential continuum background to the $\chi_c \rightarrow \pi^+\pi^-$ mode, which we expect to be under control once suitable cuts are imposed on the final-state pions. Future CEP data from the LHC and RHIC (as well as analysis from the Tevatron) will hopefully shed further light on the theory of meson pair CEP, and other exclusive processes in general.

LHL thanks the organisers for providing an excellent scientific environment at the Workshop.

References

1. C. Royon, *Acta Phys. Polon. B* **39** (2008) 2339 [arXiv:0805.0261 [hep-ph]].
2. V. A. Khoze, A. D. Martin and M. G. Ryskin, *Eur. Phys. J. C* **23** (2002) 311
3. M. G. Albrow, T. D. Coughlin and J. R. Forshaw, *Prog. Part. Nucl. Phys.* **65** (2010) 149
4. A. D. Martin, M. G. Ryskin and V. A. Khoze, *Acta Phys. Polon. B* **40** (2009) 1841
5. L. A. Harland-Lang, V. A. Khoze, M. G. Ryskin, W. J. Stirling, *Eur. Phys. J. C* **65**, 433 (2010) [arXiv:0909.4748 [hep-ph]].
6. L. A. Harland-Lang, V. A. Khoze, M. G. Ryskin, W. J. Stirling, *Eur. Phys. J.* **C69**, 179 (2010) [arXiv:1005.0695 [hep-ph]].
7. L. A. Harland-Lang, V. A. Khoze, M. G. Ryskin and W. J. Stirling, *Eur. Phys. J. C* **71** (2011) 1545 [arXiv:1011.0680 [hep-ph]].
8. L. A. Harland-Lang, V. A. Khoze, M. G. Ryskin and W. J. Stirling, *Eur. Phys. J. C* **71** (2011) 1714 [arXiv:1105.1626 [hep-ph]].
9. S. Heinemeyer *et al.*, *Eur. Phys. J. C* **71** (2011) 1649 [arXiv:1012.5007 [hep-ph]].
10. V. A. Khoze *et al.*, *Eur. Phys. J. C* **68** (2010) 125
11. R. S. Pasechnik, A. Szczurek and O. V. Teryaev, *Phys. Rev. D* **78** (2008) 014007
12. M. G. Albrow *et al.* [FP420 R & D Collaboration], *JINST* **4** (2009) T10001
13. The code and documentation are available at <http://projects.hepforge.org/superchic/>.
14. LHCb collaboration, CERN-LHCb-CONF-2011-022.
15. L. A. Harland-Lang, V. A. Khoze, M. G. Ryskin, W. J. Stirling, future publication.
16. J. W. Lamsa and R. Orava, *JINST* **4** (2009) P11019 [arXiv:0907.3847 [physics.acc-ph]].
17. V. A. Khoze, A. D. Martin, M. G. Ryskin, W. J. Stirling, *Eur. Phys. J. C* **35**, 211 (2004)
18. P. Lebiedowicz, R. Pasechnik and A. Szczurek, *Phys. Lett. B* **701** (2011) 434
19. J. Pumplin and F. Henyey, *Nucl. Phys. B* **117** (1976) 377.
20. Y. I. Azimov *et al.*, *Sov. J. Nucl. Phys.* **21** (1975) 215 [*Yad. Fiz.* **21** (1975) 413].
21. A. Breakstone *et al.* [ABCDHW Collaboration], *Z. Phys. C* **48** (1990) 569.
22. E. G. S. Luna, V. A. Khoze, A. D. Martin and M. G. Ryskin, *Eur. Phys. J. C* **59** (2009)
23. S. J. Brodsky, G. P. Lepage, *Phys. Rev.* **D24** (1981) 1808.
24. M. Benayoun, V. L. Chernyak, *Nucl. Phys.* **B329** (1990) 285.
25. V. A. Khoze, A. D. Martin and M. G. Ryskin, *Eur. Phys. J. C* **19** (2001) 477
26. S. J. Brodsky, R. W. Brown, *Phys. Rev. Lett.* **49** (1982) 966.
27. F. J. Gilman, R. Kauffman, *Phys. Rev.* **D36** (1987) 2761
28. T. Aaltonen *et al.* [CDF Collaboration], *Phys. Rev. Lett.* **108** (2012) 081801
29. A. D. Martin, W. J. Stirling, R. S. Thorne and G. Watt, *Eur. Phys. J. C* **63** (2009) 189
30. A. D. Martin, R. G. Roberts, W. J. Stirling and R. S. Thorne, *Eur. Phys. J. C* **14** (2000) 133